Fundamental characterisation of sperrylite leaching behaviour in cyanide systems using x-ray photoelectron spectroscopy

by K. Shaik[1], H. Kolev[2], Z. Cherkezova-Zheleva[2], J. Petersen[1]

Affiliation:
[1]Chemical Engineering, University of Cape Town, South Africa
[2]Institute of Catalysis, Bulgarian Academy of Sciences, Bulgaria

Correspondence to:
K. Shaik

Email:
kathija.shaik@uct.ac.za

Dates:
Received: 17 Oct. 2025
Published: February 2026

How to cite:
Shaik, K., Kolev, H., Cherkezova-Zheleva, Z., Petersen, J. 2026. Fundamental characterisation of sperrylite leaching behaviour in cyanide systems using x-ray photoelectron spectroscopy. *Journal of the Southern African Institute of Mining and Metallurgy*, vol. 126, no. 2, pp. 113–118

DOI ID:
https://doi.org/10.17159/2411-9717/930/2026

ORCiD:
K. Shaik
http://orcid.org/0000-0002-7862-2868

This paper is based on a presentation given at the 9TH International PGM Conference 2025, 27-28 October 2025, Sun City, Rustenburg, South Africa

Abstract

Sperrylite is one of the most abundant platinum minerals globally, valued for its economic importance but also known for its highly refractory nature, making it difficult to process via the conventional route. This study explores the oxidative leaching of sperrylite using a cyanide–ferricyanide system, with a key focus on characterisation of the mineral and surface speciation under varied leaching conditions using x-ray photoelectron spectroscopy. The parameters investigated include the effect of sodium cyanide concentration, the use of potassium ferricyanide as an oxidant, copper sulphate pentahydrate as a catalyst, as well as the effects of temperature and particle size. A limited set of leaching tests was carried out to study the surface chemistry rather than optimising dissolution conditions. This approach identified mineral oxidation states and shifts in binding energies, prior to and post leaching. XPS analysis of sperrylite's surface chemistry identified key species, comprising the bulk Pt(II)–As (≈73 eV) and As(–I)–Pt (≈41.8 eV) states, together with surface oxidation products Pt(II)–O (≈72 eV), Pt(IV)–O (≈74.5 eV), As(III)–O (≈43 eV) and As(V)–O (44.5 eV). Leaching led to the removal of pre-existing oxides on the ultra-finely ground sample, exposing the underlying bulk species. In contrast, the crystalline sample with an initial low concentration of oxides, generated higher amounts of fully oxidised species after leaching, reflecting greater surface reactivity.

Keywords

sperrylite, x-ray photoelectron spectroscopy, cyanide leaching

Introduction

Mining technologies are continuously advancing to reduce production costs in the competitive mining sector, while prioritising environmental sustainability (Hamrin, 2001). Mwase et al. (2012a, 2012b, 2014) developed a low-cost hydrometallurgical route using thermophilic bioleaching to extract base metals followed by cyanidation of platinum group metals (PGM). However, sperrylite ($PtAs_2$) remained largely unreacted, demonstrating its resistance to cyanide leaching under the conditions studied (Mwase, Petersen, 2017). Sperrylite displayed low solubility and required stronger oxidising conditions to achieve significant platinum (Pt) in solution. As a result, ferricyanide was introduced as an oxidant in combination with cyanide and yielded notably improved recoveries of Pt (up to 16 times) compared to a system with passive aeration. The slow leaching kinetics of sperrylite were attributed to its inherent chemical stability and surface passivation. Understanding sperrylite's dissolution required a detailed study of its surface chemistry, with the x-ray photoelectron spectroscopy (XPS) analytical technique offering a valuable means to accomplish this.

The application of XPS in studying the surface chemistry of sperrylite has been explored in a limited number of studies. Subsequent work by Mwase and Petersen (2017) demonstrated that arsenic is preferentially leached from sperrylite in a cyanide system resulting in surface enrichment of platinum and the formation of a platinum arsenide phase ($Pt–As_x$) where $x<2$. The authors went on to conclude that the formation of a passivation layer hindered further dissolution, accounting for the slow leaching kinetics observed. In contrast, Shackleton (2007) and Pikinini (2022) focused on the flotation behaviour of sperrylite, demonstrating that surface characteristics and the formation of metal oxides strongly influenced collector adsorption and recovery. Overall, these findings highlight that surface chemistry plays a key role in determining sperrylite's reactivity in both hydrometallurgical and the beneficiation process.

The reaction mechanism for sperrylite leaching is not well understood, and the oxidation states of platinum (Pt) and arsenic (As) species prior to and post leaching remain under contention. Shaik (2022) demonstrated through XPS analysis that the sperrylite sample contains platinum(II)-arsenic (Pt(II)-As), confirming platinum is in the +2 oxidation state, inferring that arsenic is likely in the -1 state. Surface and bulk As were also detected, indicating differences in arsenic distribution between the surface and the bulk of the mineral. This study focused on the oxidative leaching of a single crystalline mineral electrode and XPS analysis revealed the presence of Pt(IV) oxide, likely PtO_2. Arsenic oxides, As(III)-O and As(V)-O, were also detected on the surface, with As(V)-O becoming dominant at higher applied potentials.

In contrast to previous studies on solid mineral electrodes, the present study focuses on ultra-finely ground samples of sperrylite to gain insight into dissolution behaviour at the particle level. The objectives are to determine the oxidation states of platinum and arsenic and monitor how they evolve during leaching under varied system conditions.

Experimental

The natural sperrylite used in this study was sourced from the Sudbury Basin deposit through Wallbridge Mining Company (Canada), in collaboration with Lonmin Plc (now Sibanye-Stillwater). The mineral varied in size, with larger fragments measuring up to 3 mm and finer material extending down to -5 µm. Sub-samples of 3.5 g were micronised to achieve a particle size below 5 µm. Crystalline particle ranging from 3 mm to 4 mm in size were selected for the fabrication of electrodes. The electrode used for this specific study had a surface area of 0.0128 cm^2. X-ray diffraction (XRD) confirmed that the material was composed entirely of sperrylite. Scanning electron microscopy with energy-dispersive x-ray spectroscopy (SEM-EDS) indicated a composition of 55.13% platinum (Pt) and 44.87% arsenic (As), consistent with literature values (Henke, Hutchison, 2009). Minor impurities of copper (Cu), silicon (Si), and sulphur (S) were also detected.

All reagents used — sodium cyanide, (NaCN), potassium hexacyanoferrate(III) ($K_3[Fe(CN)_6]$), sodium carbonate (Na_2CO_3), sodium bicarbonate ($NaHCO_3$), and copper(II) sulphate pentahydrate ($CuSO_4.5H_2O$) — were of analytical grade and procured from Merck. These were used as received without further purification. Stock solutions of NaCN and $K_3[Fe(CN)_6]$ were prepared in an alkaline buffer. The standard buffer comprised 9.3 g/L Na_2CO_3 and 1 g/L $NaHCO_3$.

Leaching tests were conducted in a 500 mL reactor on a heated magnetic stirrer, ensuring continuous agitation of the solution. Approximately 0.75 g of the sperrylite mineral was used per test in 250 mL solution. For the base case, the finely ground sample was leached for 24 hours at 45°C and 500 rpm using 100 mM NaCN and 20 mM $K_3[Fe(CN)_6]$. The parameters investigated included the effect of NaCN concentration, the use of $K_3[Fe(CN)_6]$ as an oxidant, $CuSO_4.5H_2O$ as a catalyst, as well as the effects of temperature and particle size. Post leaching all samples were filtered, dried and transferred to the XPS for analysis. The ultrafinely ground sample was gently compressed into a sample stub to form a flat surface. It was handled with caution to minimise contamination and surface oxidation prior to analysis.

Ex situ x-ray photoelectron spectroscopy (XPS) measurements were performed using an ESCALAB MkII electron spectrometer (VG Scientific, now Thermo Scientific) at The Institute of Catalysis — Bulgarian Academy of Sciences (IC-BAS). The base pressure in the analysis chamber was maintained at 5 x 10^{-10} mbar, rising to 5 x 10^{-9} mbar during measurements. The system was equipped with a twin-anode, non-monochromated x-ray source (MgKα and AlKα), providing excitation energies of 1253.6 eV and 1486.6 eV, respectively. Measurements were conducted using both anodes. A pass energy of 20 eV was used for the hemispherical analyser, yielding an instrumental resolution (FWHM of the Ag $3d_{5/2}$ peak) of approximately 1 eV. Data acquired with the MgKα source were processed using SpecsLab2 and CasaXPS software (Casa Software Ltd). Spectral processing included subtraction of x-ray satellites and Shirley-type background (Shirley, 1972). Peak positions and areas were determined via symmetrical Gaussian-Lorentzian curve fitting. Relative concentrations of chemical species were calculated by normalising the peak areas to their respective photoionisation cross-sections, based on Scofield's theoretical values (Scofield, 1976).

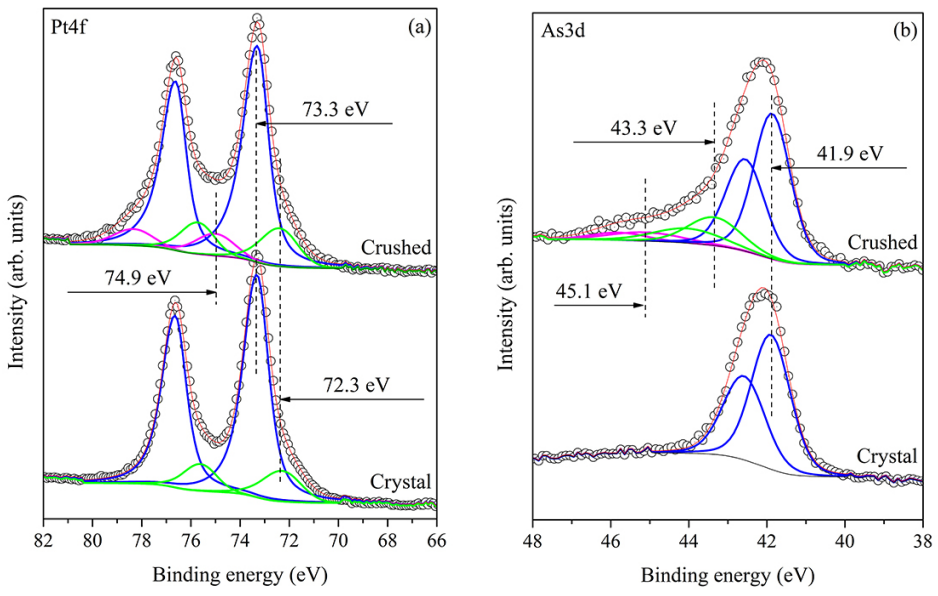

Figure 1—Pt4f and As3d XPS spectra of the untreated crystalline and ultra-finely ground sperrylite sample

Table 1

Relative proportions of the different platinum and arsenic species determined by XPS analysis

		Crystal	Ultra-finely ground
	Pt(II)-As	38.6	31.18
Pt4f	Pt(II)-O	6.47	6.38
	Pt(IV)-O	-	3.85
	As(-I)-Pt	54.93	41.58
As3d	As(III)-O	-	11.88
	As(V)-O	-	5.13

Results

Evaluation of untreated pristine crystal and ultra-finely ground sample

XPS probes only the top ~5 nm – 10 nm of the surface and this affects the species and amount detected (Briggs, Grant, 2003). For the pristine crystal sample, the surface was freshly prepared and polished to eliminate any surface products and limit exposure to air and oxidising agents. The surface remained largely unoxidised, with Pt and As retaining their original states, as reflected in the XPS spectra. As shown in Figure 1, a Pt4f peak detected at 73.3 eV was assigned to a Pt(II)-As bond, which accounted for 38.6% (Table1) of the total Pt signal. An additional peak was detected at a slightly lower binding energy of 72.3 eV assigned to Pt(II)-O and accounted for 6.47% of the relative intensity. Peaks corresponding to As3d appeared at 41.9 eV, representing 54.93% of the total signal. As the only As peak detected, it was attributed to the As (-I)-Pt. The peak assignments also took into consideration the relative proportion of the peak. In principle, oxidation of a species should lead to an increase in binding energy; this, however, was not observed for the Pt(II)–O peak. The binding energy shifts are not only dependent on oxidation state but can also be influenced by the electronegativity, bond covalency and the lattice strain, which may have contributed to the behaviour observed (Moulder et al., 1992).

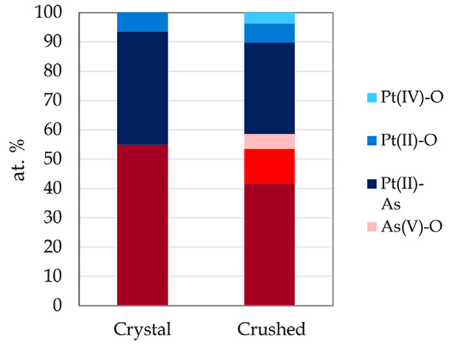

Figure 2—Relative distribution of platinum and arsenic species determined by XPS analysis

The ultra-finely ground sample generated a greater surface area, which was significantly more reactive. The physical process of crushing introduces surface defects and disrupts the metal–metal or metal–ligand bonds, creating highly reactive surface sites. Prolonged exposure to air, and other potential oxidising agents are believed to have chemically altered the surface layer. Since XPS is mostly a surface technique, it detects the oxidised layer, rather than the underlying phases. This was apparent for the ultra-finely ground sample as a greater proportion of oxidised species was detected. The Pt4f spectrum revealed a dominant peak at 73.3 eV, representing 31.18% of the total signal assigned to Pt(II)-As. A second peak at 72.3 eV, was attributed to Pt(II)–O, which displayed a relatively low intensity of 4.38%. At a further increased binding energy of 74.9 eV, oxidised Pt(IV)–O species were detected, comprising 1.85% of the total signal. The underlying bulk species, As(–I)–Pt, were detected at 41.9 eV with an intensity of 41.58%. Surface-oxidised species were also observed, with As(III)–O at 43.3 eV (11.88%) and As(V)–O at 45.1 eV (5.13%), reflecting the presence oxidised species.

Effect of various parameters

The XPS data (Figure 3) acquired for the ultra-finely ground sample under various system conditions was evaluated in relation to the untreated sample. The parameters investigated included the effect of NaCN concentration, the use of $K_3[Fe(CN)_6]$ as an oxidant, $CuSO_4.5H_2O$ as a catalyst, as well as the effects of temperature.

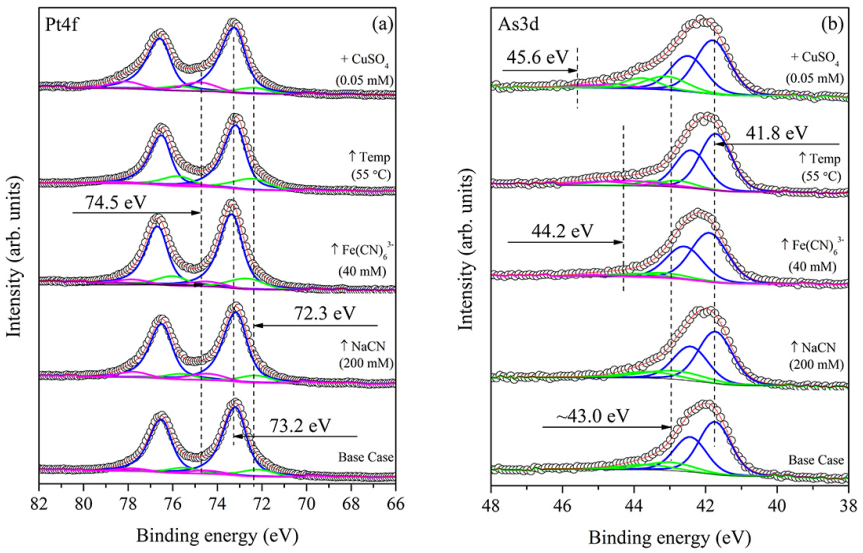

Figure 3—Pt4f and As3d XPS spectra of ultra-finely ground sperrylite under varied leach conditions

Leaching was shown to significantly modify the surface chemistry. The base case exhibited the highest relative proportion of Pt(II)-As amongst the other tests obtaining 37.47% at 73.1 eV, while the oxidised platinum species showed a marked decline compared to the untreated sample, as shown in Table 2. Pt(II)–O dropped to 3.14% at 72 eV and Pt(V)–O to 1.96% at 74.5 eV. In a similar manner the underlying bulk, As(-I)-Pt fraction, remained dominant at 46.56% (41.8 eV) and a relative intensity of 10.87% was obtained for As(III)-O at 43.1 eV.

Increasing the NaCN concentration produced similar overall trends as the base case, obtaining comparable peaks and relative intensities for the various species. The findings suggest that higher cyanide concentrations promoted the stabilisation of Pt(IV)-O and As(III)-O, yielding intensities similar to the untreated sample. As(V) was not detected in both the base case or at 200mM NaCN concentration.

As the oxidant concentration was increased to 40 mM Fe(CN), the relative proportions of Pt and As oxides declined compared to the untreated samples. The relative intensity of Pt(II)-O decreased from 6.38% to 5.64% at 72 eV. An additional peak appeared at a higher binding energy of 74.4 eV, assigned to Pt(IV)-O, showing a moderate decrease in intensity to 2.60%. Concurrently, a high relative intensity of 50.25% was detected at 41.9 eV, consistent with the As(-I)-Pt species. Minor contributions from oxidised arsenic species were also detected, comprising 6.95% As(III)–O and 2.45% As(V).

At an elevated temperature of 55 °C, a greater relative proportion of oxidised Pt species was observed. In particular Pt(II)-O displayed the highest contribution, among the parameters studied, of 7.36% (72.3 eV) and Pt(IV)-O at 1.38% (75 eV). Under the same conditions, the As(-I)-Pt fraction displayed minimal variation obtaining 45.31% at 41.7 eV. The As(V)–O peak exhibited a considerable intensity of 7.56% (44.2 eV), while As(III)-O remained at 4.72% (42.8 eV). These findings confirm that heating promotes oxidation of both arsenic and platinum species, demonstrating a more oxidising environment, likely driven by enhanced reaction kinetics.

The introduction of the catalyst resulted in a marginal increase in the oxidised species, Pt(IV)-O by 1% at 74.7 eV. The other notable change was the catalyst-induced loss of Pt(II)–O and As(V)–O, which decreased by 3.51% and 1.73%, respectively, compared with the untreated sample. The relative intensities of the underlying bulk, As(–I)–Pt and Pt(II)-As, remained largely unchanged. Overall, these results suggest that the catalyst had a negligible effect on the system.

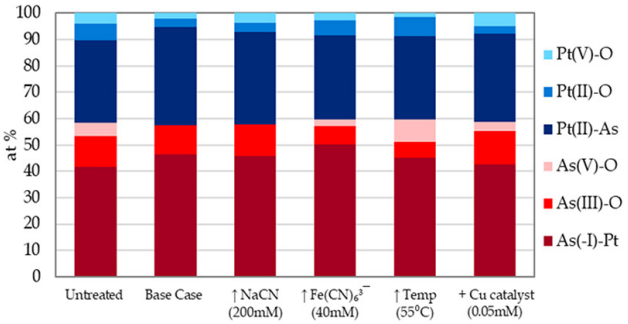

Figure 4—Relative distribution of platinum and arsenic species determined by XPS analysis under varied conditions

These results indicate that after a 24-hour leaching process, the mineral surface was not undergoing oxidation but instead dissolving the pre-existing oxidation products (Pt–O and As–O species). This allowed the exposure of the surface bulk, consistent with a process in which oxidative surface layers are stripped away rather than generated. Additionally, the surface species remained largely unchanged for the conditions studied, thus making it difficult to draw conclusive findings from the observed trends.

Effect of particle size

The effect of particle size was investigated in an ultra-finely ground (< -0.5µm), coarse (>0.5 µm to 1000 µm), and a solid crystalline sample. For the ultra-finely ground sample, leaching increased the relative proportion of Pt(II)-As by 6.29% and As (-I)-Pt by 4.98% (Figure 5), while the proportion of oxidised species marginally decreased, indicating selective removal of the surface oxides and exposure of underlying bulk. For the coarse sample, a relative intensity of 4.21% for Pt(II)-O and 5.12% for As(III)-O were detected (Table 3), while the highest proportion of As(-I)-Pt was observed at 54.84% (41.9 eV). Furthermore, highly oxidised species, Pt(IV)-O and As(V)-O were not detected on the surface, indicating that the oxidised components had likely been removed or were absent. This suggests that the coarse surface is dominated by partially oxidised species. The crystalline sample initially showed limited oxide presence. After leaching, it gained an increased proportion of oxidised species, attaining relative intensities of 1.75% for Pt(IV)–O, 6.61% for As(III)–O, and 1.51% for As(V)–O. It is believed that leaching exposed its reactive sites, leading to formation of more oxidised species.

Table 2

Relative proportions of platinum and arsenic species determined by XPS analysis under varied leach conditions

		Untreated	Base case	↑ NaCN (200 mM)	↑ $Fe(CN)_6^{3-}$ (40 mM)	↑ Temp (55 °C)	+ Cu catalyst (0.05 mM)
	Pt(II)-As	31.18	37.47	35.03	32.11	31.68	33.61
Pt4f	Pt(II)-O	6.38	3.14	3.46	5.64	7.36	2.87
	Pt(IV)-O	3.85	1.96	3.74	2.60	1.38	4.87
	As(-I)-Pt	41.58	46.56	45.75	50.25	45.31	42.61
As3d	As(III)-O	11.88	10.87	12.02	6.95	5.72	12.64
	As(V)-O	5.13	-	-	2.45	8.56	3.40

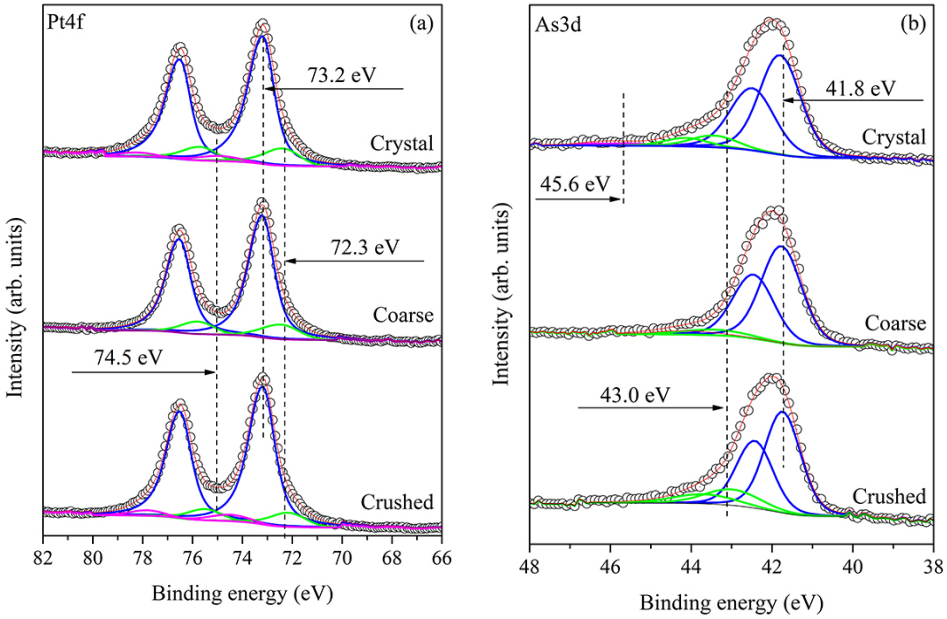

Figure 5—Pt4f and As3d XPS spectra of ultra-finely ground, coarse, and crystalline leached samples

Table 3
Relative proportions of platinum and arsenic species determined by XPS analysis across different particle sizes after leaching

		Ultra-finely ground	Coarse	Crystal
Pt4f	Pt(II)-As	37.47	35.17	34.43
	Pt(II)-O	3.14	4.93	5.18
	Pt(IV)-O	1.96	-	1.75
	As(-I)-Pt	46.56	54.84	50.52
As3d	As(III)-O	10.87	5.06	6.61
	As(V)-O	-	-	1.51

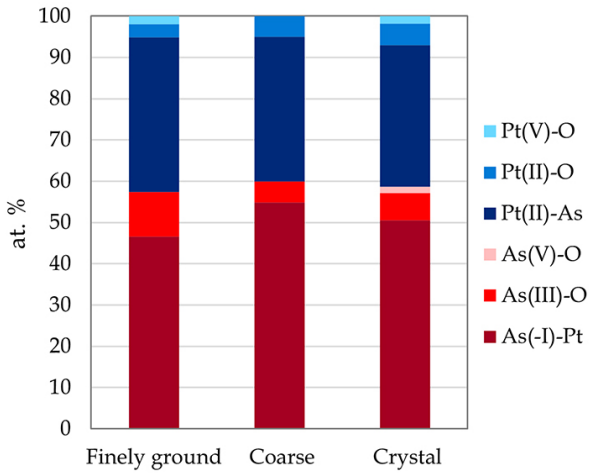

Figure 6—Relative distribution of Platinum and arsenic species determined by XPS analysis at varied particle size

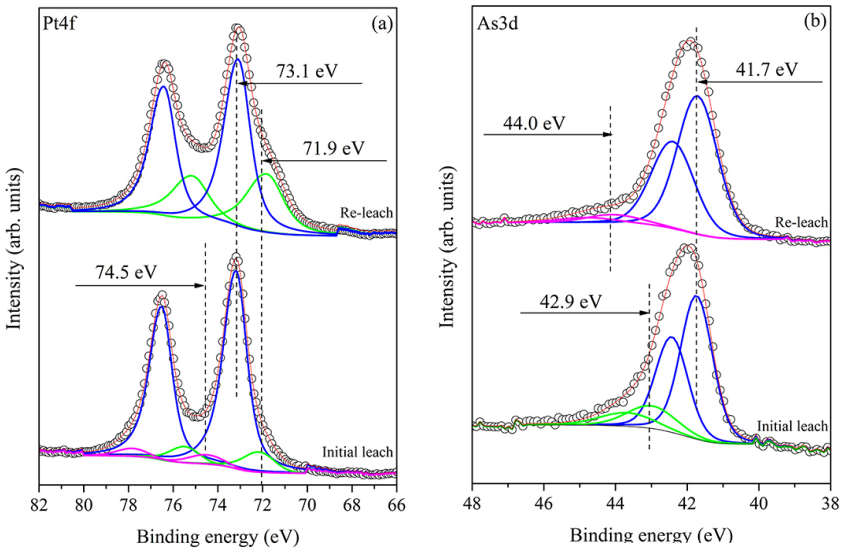

Figure 7—Pt4f and As3d XPS spectra after initial and re-leaching step

Table 4
Relative proportions of platinum and arsenic species determined by XPS analysis after initial and re-leaching steps

		Initial leach	Re-leach
	Pt(II)-As	37.47	27.63
Pt4f	Pt(II)-O	3.14	13.82
	Pt(IV)-O	1.96	-
	As(-I)-Pt	46.56	53.78
As3d	As(III)-O	10.87	-
	As(V)-O	-	4.76

Effect of re-leach

The re-leach step predominantly exposed the underlying bulk state for As(-I)-Pt obtaining a relative intensity of 53.78% at 41.7 eV (Figure 7). The relative proportion data presented in Table 4 indicates that the surface was coated with Pt(II)-O species reaching an intensity of 13.82%, with no detectable Pt(IV)-O and As(III)-O present. Pt(II)-O concentrations were exceptionally high, and arsenic was mainly stabilised as As(V) at 4.76%. This observation suggests that the oxidative species generated during the initial leach were largely consumed, creating a redox environment that stabilised Pt(II)-O and As(V) in the re-leach. The re-leach likely removed surface layers and exposed fresh material, allowing Pt(II)-O to accumulate while more highly oxidised species remained undetectable.

Conclusions

XPS analysis of sperrylite's surface chemistry identified key species, comprising the bulk Pt(II)–As (≈73 eV) and As(–I)–Pt (≈41.8 eV) states of the unoxidised sperrylite lattice, together with surface oxidation products Pt(II)–O (≈72 eV), Pt(IV)–O (≈74.5 eV), As(III)–O (≈43 eV), and As(V)–O (44.5 eV). Investigation of the various parameters after 24 hours on the ultra-finely ground sample indicated that leaching removed pre-existing Pt–O and As–O species without generating an additional oxide layer, exposing more of the underlying bulk species Pt(II)-As and As(-I)-Pt. Partially oxidised species Pt(II)-O and As(III)-O dominated amongst the oxide species found in the coarse sample, suggesting a stable surface environment favouring lower oxidation states. In contrast, the crystalline sample, with minimal oxides initially present, generated high relative proportions of the fully oxidised species (Pt(IV), As(III), and As(V)) after leaching, reflecting greater surface reactivity, leading to formation of more oxidised species. The re-leach effectively removed As(III)-O, however, the surface remained highly enriched in Pt(II)-O, suggesting incomplete removal of the oxide layer, in agreement with Mwase and Petersen (2017). This study demonstrates that the dominant oxide species and distribution depends largely on the mineral particle size and sample preparation rather than the leaching conditions itself. XPS provided valuable insights into the leaching chemistry, however, additional tests and repeated measurements are recommended to further validate the findings.

Acknowledgements

The authors also wish to acknowledge support from the European Union's Horizon 2020 Research and Innovation Programme under the MSC RISE Action 'ChemPGM' Grant Agreement No. 101007669.

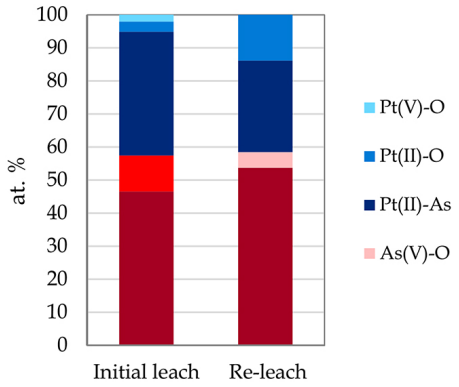

Figure 8—Relative distribution of platinum and arsenic species determined by XPS analysis after initial and re-leach step

References

Briggs, D., Grant, J.T. 2003. *Surface Analysis by Auger and X-ray Photoelectron Spectroscopy*. IM Publications.

Hamrin, H. 2001. Underground mining methods and applications, in W. A. Hustrulid and R. L. Bullock (eds), *Underground Mining Methods: Engineering Fundamentals and International Case Studies.* Littleton: Society for Mining, Metallurgy, and Exploration, pp. 3–14.

Henke, K.R., Hutchison, R.A. 2009. *Surface oxidation of sperrylite and its impact on flotation. Minerals Engineering*, vol. 22, pp. 1012–1018.

Mwase, J.M., Petersen, J., Eksteen, J.J. 2012. *A conceptual flowsheet for heap leaching of platinum group metals (PGMs) from a low-grade ore concentrate. Hydrometallurgy*, vol. 1, pp. 111–112, 129–135.

Mwase, J.M., Petersen, J., Eksteen, J.J. 2012. *Assessing a two-stage heap leaching process for Platreef flotation concentrate. Hydrometallurgy*, pp. 129–130, 74–81.

Mwase, J.M., Petersen, J., Eksteen, J.J. 2014. A novel sequential heap leach process for treating crushed Platreef ore. *Hydrometallurgy*, vol. 141, pp. 97–104.

Mwase, J. Petersen, J. 2017. Characterizing the leaching of sperrylite ($PtAs_2$) in cyanide-based solutions. *Hydrometallurgy*, vol. 172, pp. 1–10. doi:10.1016/j.hydromet.2017.06.019

Moulder, J.F., Stickle, W.F., Sobol, P.E., Bomben, K.D. 1992. *Handbook of X-ray Photoelectron Spectroscopy*. Eden Prairie, MN: Perkin-Elmer Corporation.

Pikinini, S. 2022. An investigation into the flotation response of sperrylite ($PtAs_2$) *by comparative evaluation of crystal structure and bonding atoms*. PhD thesis. University of Cape Town. Available at: http://hdl.handle.net/11427/37701

Scofield, J.H. 1976. Theoretical photoionization cross sections from 1 to 1500 keV. *Journal of Electron Spectroscopy and Related Phenomena*, vol. 8, p. 129. https://doi.org/10.2172/4545040

Shackleton, N.J., Malysiak, V., O'Connor, C.T. 2007. Surface characteristics and flotation behaviour of platinum and palladium arsenides. *International Journal of Mineral Processing*, vol. 85, pp. 1–3, pp. 25–40. doi:10.1016/j.minpro.2007.08.002 SAIMM

Shaik, K. 2022. *Investigation of the electrochemical dissolution of sperrylite in cyanide-ferricyanide systems*. PhD thesis. University of Cape Town.

Shirley, D.A. 1972. High-resolution X-ray photoemission spectrum of the valence bands of gold. *Physical Review B*, vol. 5, pp. 4709–4714. https://doi.org/10.1103/PhysRevB.5.4709 ◆